Supporting information

Synthesis of $Au_{130}(SR)_{50}$ and $Au_{130-x}Ag_x(SR)_{50}$ Nanomolecules through Core Size Conversion of Larger Metal Clusters

Vijay Reddy Jupally, Amala Dass*

Department of Chemistry and Biochemistry, University of Mississippi, University, MS 38677. amal@olemiss.edu

Table S1: Reproducibility table showing several reactions performed with varying ligands to check the core size conversion process. In all the cases $Au_{130}(SR)_{50}$ is being observed.

#	Name of the reaction	Ligand	Upon etching
1	VJ2-65-A-ET	Phenylethanethiol	Au_{130} observed
2	VJ2-75-A-ET	Phenylethanethiol	Au_{130} observed
3	VJ2-87-B-ET	Phenylethanethiol	Au_{130} observed
4	VJ2-89-A-ET	Phenylethanethiol	Au_{130} observed
5	VJ2-92-A-ET	hexanethiol	Au_{130} observed
6	VJ2-99-B-ET	AuAg, phenylethanethiol	Ag-Au_{130} observed
7	VJ2-100-A-ET	Hexanethiol	Au_{130} observed
8	VJ2-100-B-ET	Phenylethanethiol	Au_{130} observed
9	VJ2-125-A-ET	Phenylethanethiol	Au_{130} observed
10	VJ2-135-B-ET	AuAg, phenylethanethiol	Ag-Au_{130} observed
11	VJ2-142-A-ET	Phenylethanethiol	Au_{130} observed
12	VJ2-150-B-ET	Dodecanethiol	Au_{130} observed
13	VJ2-152-B-ET	Hexanethiol	Au_{130} observed
14	VJ2-153-B-ET	AuAg, Phenylethanethiol	Au_{130} observed
15	VJ2-153-C-ET	Hexanethiol	Au_{130} observed
16	VJ2-156-C-ET	Phenylethanethiol	Au_{130} observed
17	VJ3-10-D-ET	Dodecanethiol	Au_{130} observed
18	VJ3-13-E-ET	Au,Pd Phenylethanethiol	Au_{130} observed
19	VJ3-43-B-ET	Phenylethanethiol	Au_{130} observed
20	VJ3-43-C-ET	Hexanethiol	Au_{130} observed

21	VJ3-47-B-ET	Phenylethanethiol	Au_{130} observed
22	VJ3-47-C-ET	Hexanethiol	Au_{130} observed
23	VJ3-53-A-ET	Dodecanethiol	Au_{130} observed
24	VJ3-66-A-ET	Phenylethanethiol	Au_{130} observed
25	VJ3-85-A-ET	Phenylethanethiol	Au_{130} observed
26	VJ3-85-B-ET	Hexanethiol	Au_{130} observed

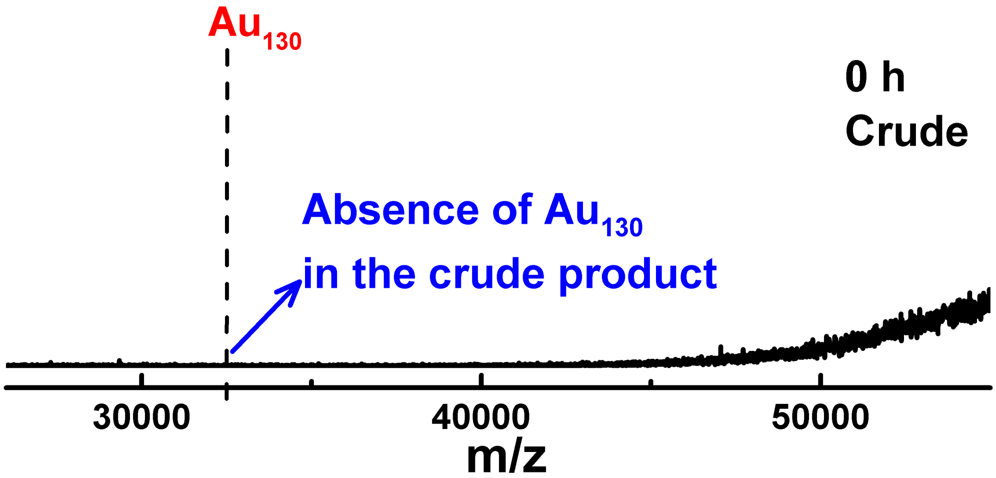

Figure S1: 0 h product from Figure 1 in the mansucript, expanded in 32 kDa mass region showing the absence of any $Au_{130}(SCH_2CH_2Ph)_{50}$.

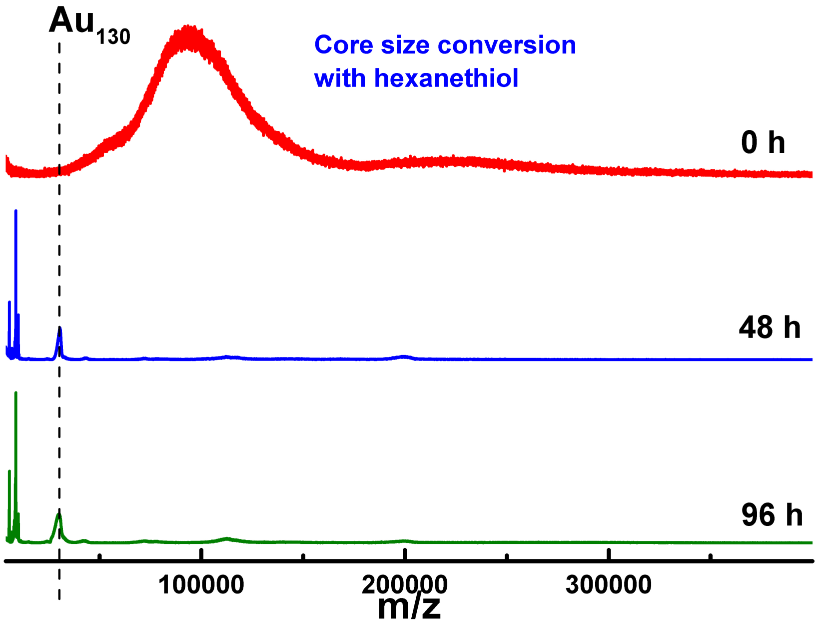

Figure S2: MALDI mass spectra of the samples collected from the etching reactions with *hexanethiol* clusters.

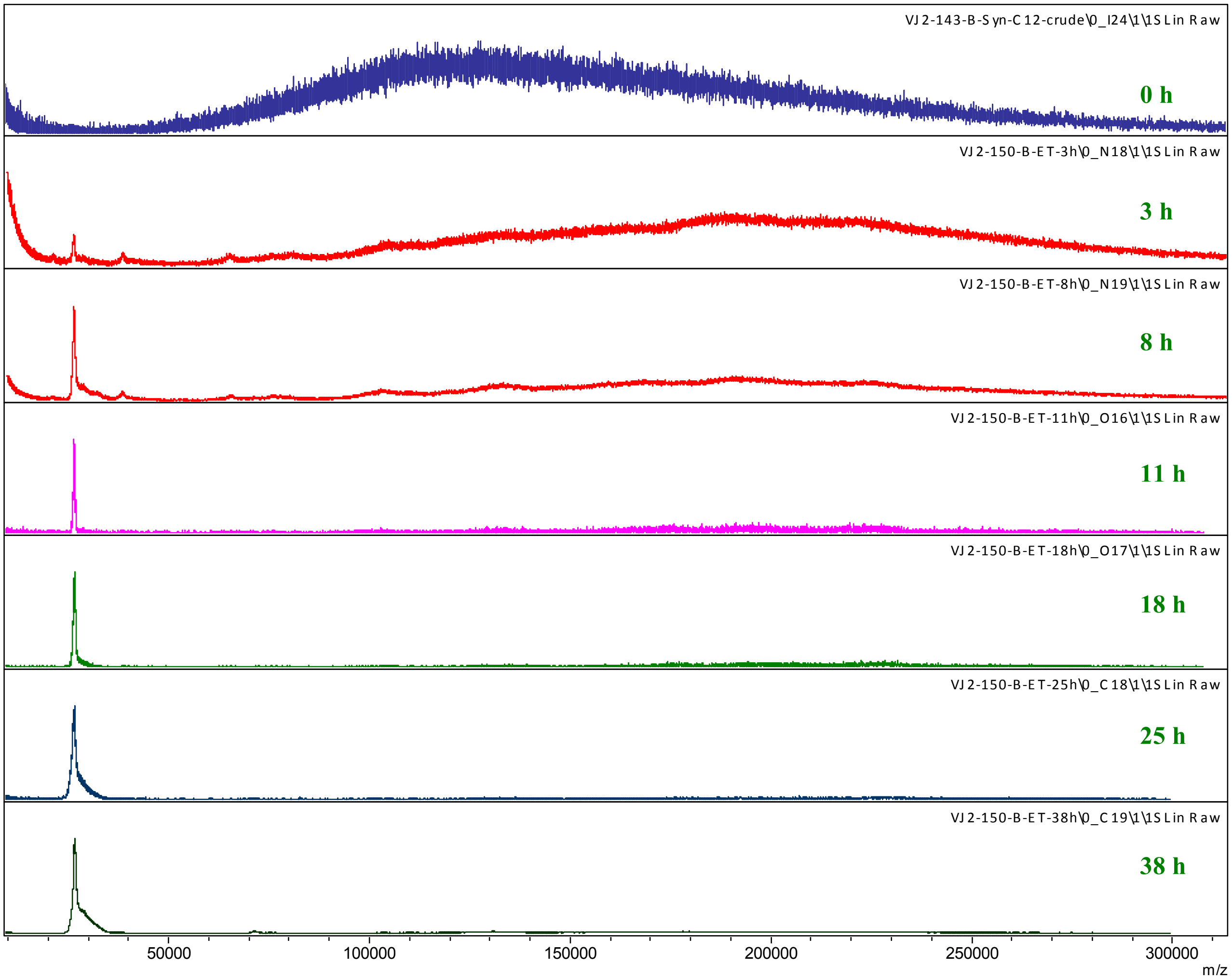

Figure S3: MALDI mass spectra of the samples collected from the etching reactions with *dodecanethiol* clusters.

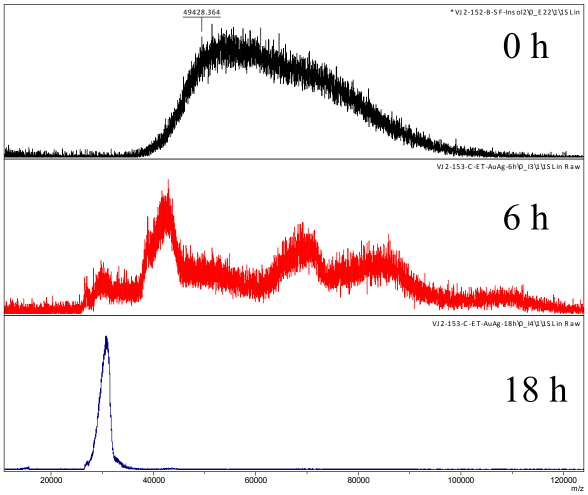

Figure S4: MALDI mass spectra of the samples collected from the etching reactions with *Au-Ag alloy* clusters.

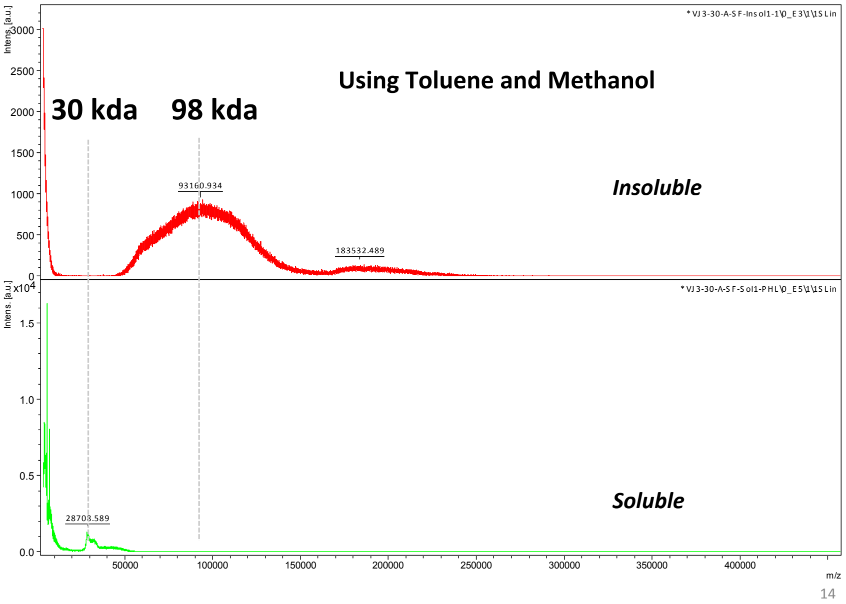

Figure S5: MALDI mass spectra of the fractions obtained from solvent fractionation steps to isolate larger clusters. The insoluble fraction (top) was used for etching reaction to obtain 130-atom species. The soluble fraction (bottom) contains Au144 species, which were removed and discarded. Since 144-atom was removed, the difficult 144- and 130-atom separation is not necessary.

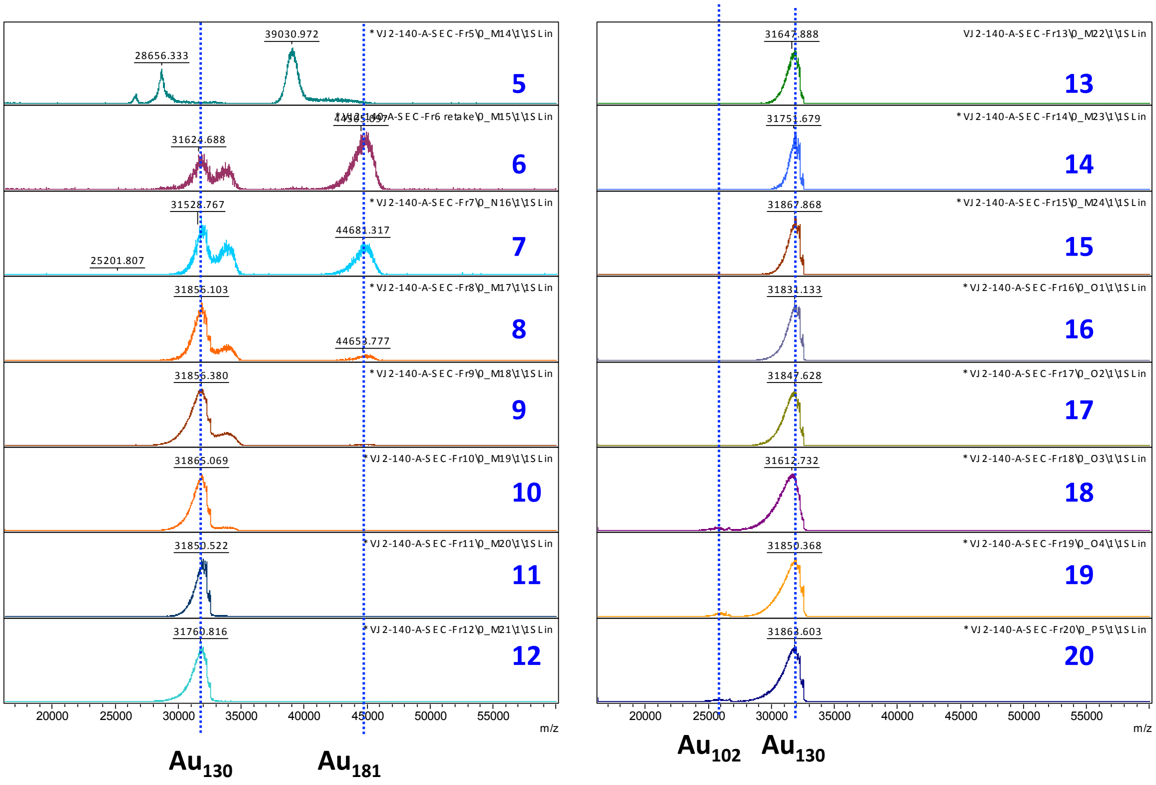

Figure S6: MALDI mass spectra of several fractions isolated from size exclusion chromatography.

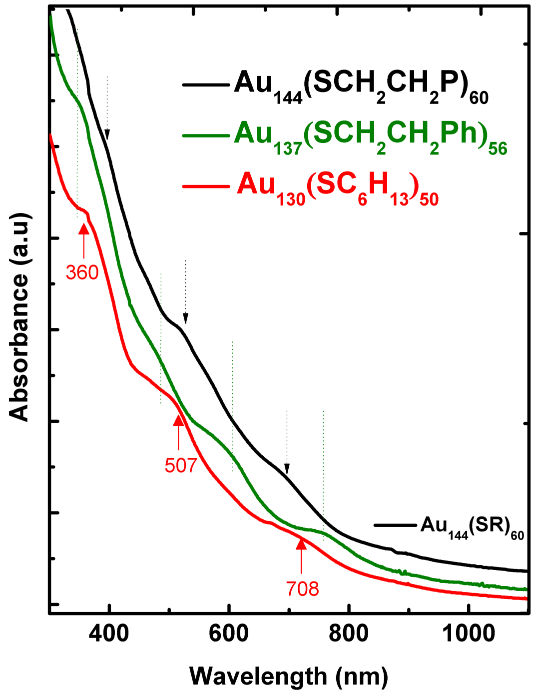

Figure S7: UV-vis spectrum of $Au_{130}(SR)_{50}$ (red) in comparison with $Au_{137}(SR)_{56}$ (green) and $Au_{144}(SR)_{60}$ (black).

Optical features of nanomolecules are often dictated by the metallic core in nanomolecules. The reason for different absorbance features of Au_{144}, Au_{137} and Au_{130} might be due to the differences in the atomic arrangements of the metal core.

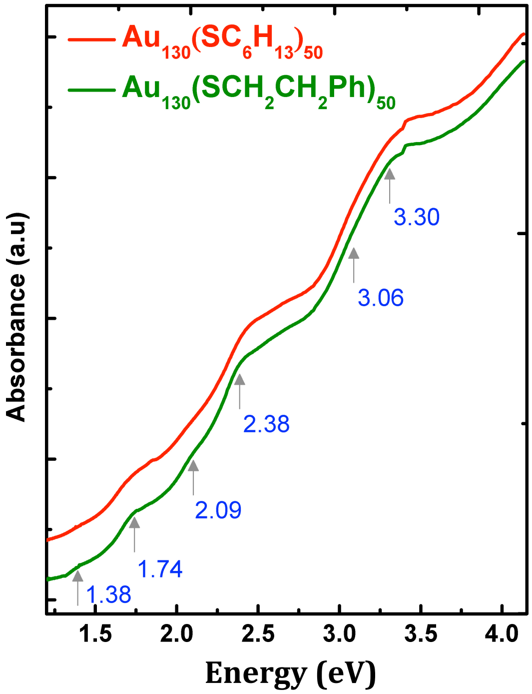

Figure S8: UV-vis spectra of $Au_{130}(SR)_{50}$ with phenylethanethiol and hexanethiol ligands in energy scale. The optical features of match with each other even though the ligand is varied.

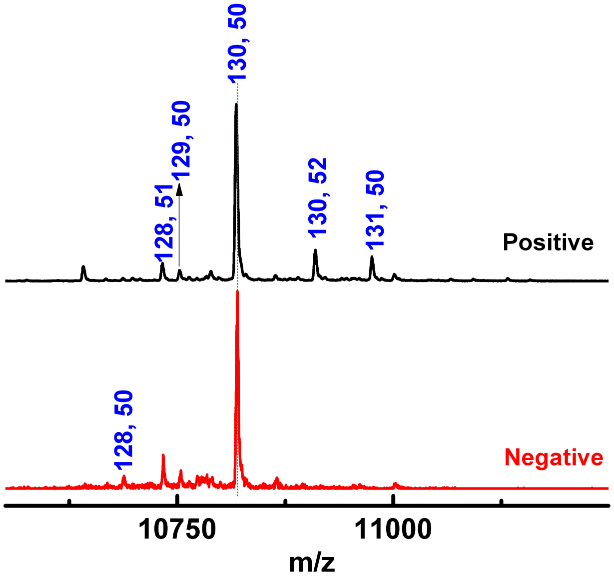

Figure S9: Positive and negative mode ESI-MS data for $Au_{130}(SCH_2CH_2Ph)_{50}$ indicating that no counter ions are present. The numbers represent the number of gold atoms and ligands respectively. To be noted, 129, 50 and 128,50 are also reported by Negishi and coworkers.

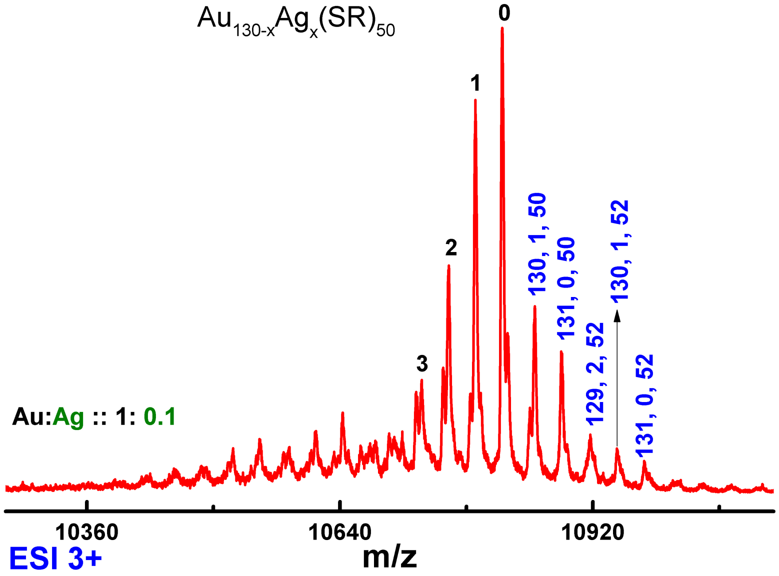

Figure S10: Postive ESI MS spectrum of $Au_{130-x}Ag_x(SCH_2CH_2Ph)_{50}$ in 3+ charge state. The peaks to the left are assigned to show the number of gold atoms, silver atoms and ligands respectively. To be noted 131, 0, 52 type cluster is not observed without silver incorporation.

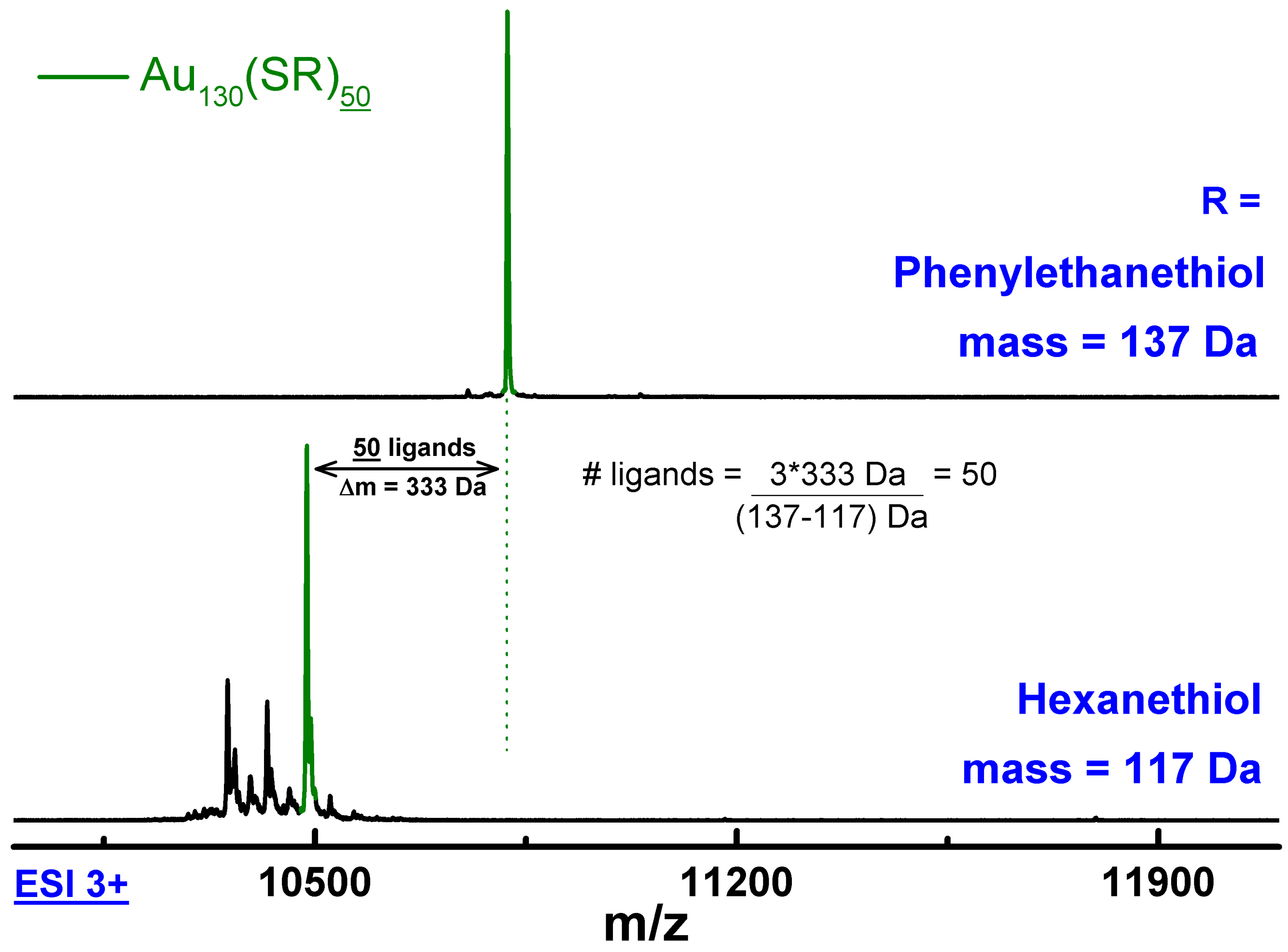

Figure S11: Positive ESI MS spectrum of $Au_{130}(SCH_2CH_2Ph)_{50}$ and $Au_{130}(SC_6H_{13})_{50}$ in 3+ charge state. The difference in the mass of these peaks is used to calculate the number of ligands in the composition.

In figure S11, the olive peaks correspond to $Au_{1130}(SR)_{50}$ nanomolecule species in both the spectra. In the top and bottom spectra phenylethanethiol and hexanethiol are the ligands respectively. The difference in the mass of these peaks is 333 Da. But, the peaks observed here have 3+ charge. This means that the actual mass difference is 333 * 3 = 999 Da.

The two olive peaks (top and bottom spectra) have the same compostion. Thus, they should have the same number of metal atoms and ligands. As the mass contribution by gold atoms is same in both the cases, the observed mass difference should be because of the ligands.

The mass difference between phenylethanethiol and hexanethiol ligands is 137 Da – 117 Da = 20 Da. Thus, the number of ligands in the nanomolecule is given by

# of ligands = total mass difference / mass difference of the ligands

In this case,
# of ligands = 999 / 20 = 49.95 ~ 50 ligands.

II. Optimization of synthetic conditions to improve the yield of $Au_{130}(SR)_{50}$

Crude product synthesis:

For synthesizing $Au_{130}(SR)_{50}$ by the process of core conversion, clusters larger than $Au_{144}(SR)_{60}$ are needed. To get majority of the nanomolecule population in this size regime, the gold : thiol ratios were optimized. After trying several ratios, 1:1, 1:0.5, 1:0.25 gold:thiol ratios for phenylethanethiol, hexanethiol and dodecanethiol respectively were found to give desired size distribution. For making composomers using Ag and Pd, 1:0.1 Au:Ag/Pd ratio was used, while gold:thiol ratio was kept the same.

Isolation of larger clusters:

Using optimized gold : thiol ratios, there are still some clusters < 40 kDa. Solvent fractionation was used to remove these species from the sample. Toluene/THF and methanol were the solvent of choice. There are two primary reasons for eliminating clusters < 40 kDa prior to etching. 1) $Au_{144}(SR)_{60}$ and $Au_{137}(SR)_{56}$ interfere with $Au_{130}(SR)_{50}$ during size exclusion chromatography. Though this seems trivial, much difficulty is involved in separating these three species. Separation may take several cycles of SEC which involves material loss, efforts and time. 2) Also, absence of these clusters would make the core size conversion clearly evident.

Core size conversion:

The precipitate obtain from solvent fractionation was etched with excess thiol at 85^{o}C$^{\cdot}$ The reactions are monitored by collecting samples at different time intervals and analyzing them by MALDI-TOF mass spectrometry. Reactions were stopped when most of the larger clusters have core converted to $Au_{130}(SR)_{50}$. It should be noted that the reaction time varies for different batches.

Isolation by SEC:

After etching, the samples obtained contain other larger nanomolecules. This includes recently reported 76 kDa faradaurate nanomolecule. For isolating highly pure $Au_{130}(SR)_{50}$ nanomolecules previously reported SEC methods were employed.

References

(1) Brust, M.; Walker, M.; Bethell, D.; Schiffrin, D. J.; Whyman, R. *J. Chem. Soc., Chem. Commun.* **1994**, 801.
(2) Knoppe, S.; Boudon, J.; Dolamic, I.; Dass, A.; BuÃàrgi, T. *Anal. Chem.* **2011**, *83*, 5056.
(3) Negishi, Y.; Sakamoto, C.; Ohyama, T.; Tsukuda, T. *J. Phys. Chem. Lett* **2012**, *3*, 1624.